Monolayer arrangement of fatty hydroxystearic acids on graphite: Influence of hydroxyl groups

S. Medina [1], *J. J. Benítez*[2], *M. A. Castro*[2], *C. Cerrillos*[3], *C. Millán*[2], *M. D. Alba*[2,*]

[1]Laboratorio de Rayos-X, Centro de Investigación Tecnología e Innovación de la Universidad de Sevilla (CITIUS), Universidad de Sevilla, Avenida Reina Mercedes, 4B. 41012 Sevilla. Spain.

[2]Instituto de Ciencia de Materiales de Sevilla
Consejo Superior de Investigaciones Científicas-Universidad de Sevilla
Avenida Américo Vespucio, 49. 41092 Sevilla. Spain.

[3]Servicio de Microscopía, Centro de Investigación Tecnología e Innovación de la Universidad de Sevilla (CITIUS), Universidad de Sevilla, Avenida Reina Mercedes, 4B. 41012 Sevilla. Spain.

ABSTRACT

Previous studies have indicated that long-chain linear carboxylic acids form commensurate packed crystalline monolayers on graphite even at temperatures above their melting point. This study examines the effect on the monolayer formation and structure of adding one or more secondary hydroxyl, functional groups to the stearic acid skeleton (namely, 12-hydroxystearic and 9,10-dihydroxystearic acid). Moreover, a comparative study of the monolayer formation on recompressed and monocrystalline graphite has been performed through X-ray Diffraction (XRD) and Scanning Tunneling Microscopy (STM), respectively. The Differential Scanning Calorimetry (DSC) and XRD data were used to confirm the formation of solid monolayers and XRD data have provided a detailed structural analysis of the monolayers in good correspondence with obtained STM images. DSC and XRD have demonstrated that, in stearic acid and 12-hydroxystearic acid adsorbed onto graphite, the monolayer melted at a higher temperature than the bulk form of the carboxylic acid. However, no difference was observed between the melting point of the monolayer and the bulk form for 9,10-dihydroxystearic acid adsorbed onto graphite. STM results indicated that all acids on the surface have a rectangular *p2* monolayer structure, whose lattice parameters were uniaxially commensurate on the *a*-axis. This structure does not correlate with the initial structure of the pure compounds after dissolving, but it is conditioned to favor a) hydrogen bond formation between the carboxylic groups and b) formation of hydrogen bonds between secondary hydroxyl groups, if spatially permissible. Therefore, the presence of hydroxyl functional groups affects the secondary structure and behavior of stearic acid in the monolayer.

Keywords. Graphite, carboxylic acid, monolayer, solid-liquid interface, VT-XRD, DSC, STM.

1. Introduction

Physisorption of organic liquids to a solid surface has been widely investigated because the layers formed at the surface affects the surface properties and allows understanding the processes important in many areas, including wetting, detergents, lubricants and other surface agents [1]. Among the substrates tested, graphite is a good substrate as it will not chemically bond or create stronger intermolecular interactions than van der Waals forces with the adsorbate molecules. The intermolecular interactions within the adsorbed monolayer are therefore the most significant forces present [2,3].

Nowadays, the literature continues to highlight the importance of detailed crystal structures in understanding the behavior of adsorbed monolayers in a wide variety of situations [4]. The formation of ordered, adsorbed monolayers of alkanes, alcohols and acids was demonstrated through delicate dilatometric and calorimetric studies [5,6]. Carboxylic acids have been reported to form close-packed crystalline monolayers on graphite even at temperatures above the bulk melting point of the acid, and those of 14 to 20 carbon atoms in length (C14 - C20) were reported as producing well-developed monolayers with strongly hydrogen-bonded dimers [7,8,9].

The majority of acids studied have even numbers of carbon atoms and were found to form slightly oblique unit cells with plane group *p2* and which exhibit a positional correlation with the underlying graphite [7,8,9]. The alkyl chains interdigitate and there is a superstructure in the direction perpendicular to the chains with a repeat distance of four or five molecules. The odd members that have been studied [7], such as heptadecanoic (C17) and nonadecanoic (C19) acid, were reported to exhibit a different *pgg* symmetry and rectangular unit cell. Rabe et al. [10], who studied stearic (C18), arachidic (C20), and tetracosanoic (C24) acids, concluded that the mismatch parameter between the side-by-side separation of alkyl chains and the graphite lattice is approximately 10%.

In most cases, the structure of carboxylic acid monolayers on graphite has been resolved by scanning tunneling microscopy. More recently, X-ray and neutron diffraction have been used to

study such solid crystalline monolayers [4]. However both techniques introduce some difficulties. Neutron diffraction can only by carried out at few specific facilities around the world. On the other side, X-ray diffraction of monolayers deposited on graphite substrates shows serious transmission problems that restrict its application only to sub-monolayer regimes. In this article we use an experimental setup that makes the monolayer diffraction studies accessible to relatively conventional XRD diffractometers. This methodology has been previously employed to study mixture undecanoic-dodecanoic acid adsorbed on graphite surface at submonolayer regime [11].

This present work is a comprehensive combination of calorimetry measurements (DSC), XRD and scanning tunnel microscopy (STM) forming an in depth study into the behavior and structure of stearic and hydroxystearic acids adsorbed onto graphite surfaces. Here, we study the adsorption structures of the pure acids from their liquids and compare the results with the structure of the bulk acids. X-ray diffraction data are used to confirm the formation of solid monolayers and provide a detailed structural analysis of the monolayers formed by each of the acids under investigation. STM is the main technique employed for characterizing surface structures of self-assembled monolayer and gives many insights into the structure and dynamics of such monolayers [12,13,14]. Visualization on the atomic scale of molecular structures in real space is extremely helpful for understanding self-assembly processes, plus the solid-liquid interface is an excellent environment in which to probe them [15,16,17].

2. Experimental details

2.1 Materials

Two substrates were used in these experiments. Recompressed exfoliated graphite Papyex (Le Carbone Lorraine, France) [18] for X-ray Diffraction and Differential Scanning Calorimetry (DSC) experiments and a highly ordered pyrolytic graphite (HOPG) (SPI Supplies, USA) for Scanning

Tunneling Microscopy (STM). The specific surface area determined by nitrogen adsorption is 31.6 $m^2 \cdot g^{-1}$ for the graphite used in XRD and DSC and $4.8 \cdot 10^{-4}$ $m^2 \cdot g^{-1}$ for HOPG.

The adsorbates were stearic acid ($C_{18}H_{36}O_2$, CAS: 57-11-4), 12-hydroxystearic acid ($C_{18}H_{36}O_3$, CAS: 106-14-9) and erythro-9,10-dihydroxystearic acid ($C_{18}H_{36}O_4$, CAS: 3639-32-5) obtained from Sigma Aldrich at 99% purity and used without further purification.

The solvents used for STM sample preparations were phenyloctane ($C_{14}H_{22}$, CAS: 2189-60-8) for dissolving stearic acid and 12-hydroxystearic acid and octanol ($C_8H_{18}O$, CAS: 111-87-5) for dissolving 9,10-dihydroxystearic acid.

2.2 Sample preparation

The pure stearic acid, stearic, 12-hydroxystearic acid and 9,10-dihydroxystearic acid, without graphite were studied as provided, after heating at 150 ºC and cooling down up to room temperature, after drying at 25 ºC a 5-10 $mg \cdot cm^{-3}$ solution of the stearic and 9,10-dihydroxystearic acid in octanol and 12-hydroxystearic acid in phenyloctane, and, after drying at 25 ºC a 5-10 $mg \cdot cm^{-3}$ solution of the 150 ºC heated stearic acid and 9,10-dihydroxystearic acid in octanol and 150 ºC heated 12-hydroxystearic acid in phenyloctane.

The graphite substrates used for diffraction and calorimetry were outgassed under vacuum in an oven at 350 ºC. Subsequently, a known quantity of the adsorbates were added and annealed at a temperature of 150 ºC, below the bulk boiling point.

Total coverage was maintained at 0.9 or 3 monolayers for XRD and 60 monolayers for DSC experiments. The volumes of adsorbate required to achieve the desired level of deposition were taken from the area per molecule values of 122 $Å^2$/molecule for stearic acid, 129 $Å^2$/molecule for 12-hydroxystearic acid and 135 $Å^2$/molecule for 9,10-dihydroxystearic acid, estimated using the Groszek model [19,20] and the specific surface area of the graphite.

The surface of HOPG used for STM measurements was cleaned by cleaving with an adhesive tape. A drop of the solution (approx. 5-10 $mg.cm^{-3}$) was immediately deposited on the support and allowed for stabilizing at 25 ºC for 5-10 minutes before STM analysis.

123

124 *2.3 Experimental procedures*

125

126 X-ray diffraction measurements of pure acids were carried out in a Bruker D8 Advance A25
127 diffractometer (Bruker, Germany) in Bragg-Brentano configuration. The detector used was a
128 Lynxeye PSD detector (Bruker, Germany), with a 0.5º fix slit in the incident beam and axial Soller
129 slits of 2.5º in the incident and diffracted beams, for copper Kα radiation, at Centro de Investigación
130 Tecnología e Innovación de la Universidad de Sevilla (CITIUS). Measurements were taken with a
131 2θ range between 3º and 120º, a step of 0.015º and a time per step of 0.1 s.

132 Variable temperature X-ray diffraction (VTXRD) of the acids adsorbed onto graphite were
133 carried out in an Anton Paar TTK 450 low-temperature chamber (Anton Paar, Austria) attached to a
134 Bruker D8 Advance diffractometer (Bruker, Germany), modified for symmetrical transmission
135 geometry [21] at CITIUS, University of Sevilla, Spain. Single rectangular sheets of graphite, with
136 dimensions of approximately 15 × 30 × 2 mm and 1 g, were irradiated by copper Kα radiation. The
137 device uses θ/θ X-ray tube and detector movement to maintain the momentum transfer in the plane
138 of the graphite sample. Experiments were performed with parallel Johansson geometry in the
139 incident beam, using 60 mm Göbel mirrors (Bruker, Germany) for copper Kα radiation. The
140 experiments were carried out at a total coverage of 0.9 and 3 monolayers for the three adsorbed acids
141 with a 2θ range between 17º and 24º, a step of 0.015º and a time per step of 10 s. The detector used
142 was a Vantec PSD detector (Bruker, Germany) with radial Soller slits. The temperature range for the
143 measurements was between 25 and 125 ºC, obtaining the patterns with a temperature step of 10 ºC
144 when far from the bulk melting point and in steps of 1 ºC when near to the bulk and monolayer
145 melting temperatures.

146 Both diffractometers were calibrated mechanically according to the manufacturer
147 specifications and corundum and silicon standards were used to check the resolution in a wide range
148 of angles.

149 The Differential Scanning Calorimetry (DSC) measurements were performed on a Thermal
150 Analysis Instrument Q20P systems at the Instituto de Ciencia de los Materiales de Sevilla, Spain, as
151 discussed previously [22]. The temperature range was from 30 to 200 ºC. The rate of heating was 10
152 $ºC \cdot min^{-1}$.

153 The Scanning Tunneling Microscopy (STM) images of the liquid-solid interface were taken
154 at room temperature, using Pt/Ir 80:20% mechanically cut tips. Two microscopes were used, a
155 Topometrix Discoverer with a scanner of 1.5 x 1.5 μm^2 at the Instituto de Ciencia de los Materiales
156 de Sevilla (CSIC-US) and a Molecular Imaging with a scanner of 1 x 1 μm^2 at CITIUS, University
157 of Sevilla, Spain. They were operated in constant height mode, using sample negative bias voltages
158 ranging from -0.12 to -1.2 V. For 1-octanol, a strong ionic background current was detected and the
159 set point was modified accordingly. The molecular packing structure was only obtained at a very low
160 and very narrow range of tunneling current. Higher set points meant the immediate observation of
161 the underlying graphite pattern which was used for in-situ X and Y calibration.
162
163 *2.4 Calculations for determining the structural parameters of the adsorbed materials*
164
165 Since not all of the structural parameters of the three materials adsorbed onto graphite have
166 previously been reported, the parameters that are lacking have been determined using structural
167 parameters published for other carboxylic acids [4] with shorter chains in other studies that explain
168 how the carboxylic acids [7] and 12-hydroxystearic acid [23] adsorbed onto graphite. The position of
169 the atoms was deduced from the data published for undecanoic acid [4]; stretching and filling the
170 molecular structure up to an eighteen-carbon chain with the corresponding hydrogen and oxygen
171 atoms in their positions, including the hydroxyl or dihydroxyl groups of the branched-chain acids.

172 Previously deduced structures were verified by superimposing the above schematic STM
173 images obtained for the three acids adsorbed on graphite. The diagrams showing the molecular
174 structures were produced using the ATOMS programme, by Shape Software (Eric Dowty, USA).
175

3. Results and discussion

3.1 Polymorphic transitions of pure acids

This section characterizes the bulk of the material in absence of graphite. Fig. 1a shows the XRD patterns of the pure acids. They were completely different depending on the presence of one or more hydroxyl groups on the alkyl chain. The Le Bail [24] fits of the patterns were performed with the software TOPAS 4.2 from Bruker [25] (Tables 1-3) using the fundamental parameters method. The zero error (2θ), the sample displacement, the absorption (1/cm) and the lattice parameters of the phases were allowed to vary to provide the best fitting. The background was fitted by a fifth-order Chebychev polynomial. Lorentz and polarization geometric factors for the configuration of measurement were used. From the fits was revealed that the stearic acid XRD pattern (Fig. 1a, upper) matches with the polymorph B_o (orthorhombic, *Pbca*) [26] whereas, 12-hydroxystearic and 9,10-dihydroxystearic acids match with polymorphs A (triclinic, *P1*) [27] and E_o (orthorhombic, *Pbca*) [28], respectively. Overall a good residue was obtained as the difference between the calculated value and the experimental value for all cases. For the fit to be as accurate as possible the GOF ("Goodness of fit") should be greater than 1, and as close as possible to it [29]. Another parameter to note is the experimental residue (Rwp), which must have a value as small as possible for the measurement configuration used [29]. Good fit values were obtained.

An in depth analysis of the polymorph's stability with respect to temperature and solvent type has been carried out using the Le Bail fit from each of the XRD patterns (Fig. 1 and Tables 1-3). The analysis reveals that, for stearic acid (Fig. 1, upper), the polymorph B_o is transformed into polymorph C (monoclinic, $P2_1/a$) [30] by heating to 150 ºC or by dissolving in phenyloctane. After heating to 150 ºC, the polymorph C in the phenyloctane solution evolved into a mixture of the polymorphs C and B_o, accompanied by an amorphous phase that is probably due to incomplete recrystallization of the polymorphs. With time, the latter evolved to a polymorph C as the most stable phase and the amorphous phase decreased significantly (Fig. 2, upper).

The polymorph A of 12-hydroxystearic acid (Fig. 1, middle) was stable after heating to 150 ºC and dissolving in phenyloctane. However, heating the solution to 150 ºC produced a small amount of amorphous phase that may indicate that the recrystallization of the polymorph A is a reconstructive process.

In the case of 9,10-dihydroxystearic acid (Fig. 1, bottom), the polymorph E_o was transformed into polymorph C by heating to 150 ºC. The polymorph E_o was stable after dissolving in octanol but, after heating to 150 ºC, it evolved into a mixture of the polymorphs C and E_m (monoclinic, $P2_1/a$) [31] plus an amorphous phase due to the incomplete recrystallization of the polymorphs. The latter mixture evolved to a polymorph C with time as a more stable phase and the quantity of the amorphous phase decreased significantly (Fig. 2, bottom).

3.2 Formation of acid monolayers on graphite surfaces

Fig. 3 shows the DSC thermograms for approximately 60 monolayers of the acids adsorbed on graphite. Stearic acid and 12-hydroxystearic acid (Fig. 3a and 3b) exhibited a very large peak at a temperature of 65 - 80 ºC corresponding to the bulk melting point of the acid. Note, at this high coverage the temperature of the bulk transitions are identical whether graphite is present or not (Table 4). Additionally, a small peak was observed at 95 - 100 ºC that arises from the melting of the adsorbed monolayer that coexisted with the bulk liquid at this temperature. The DSC plot of 9,10-dihydroxystearic acid adsorbed on graphite (Fig. 3c) showed only a wide peak at a temperature of 129.5 ºC due to the complete melting of the acids. These results could imply that the monolayer, if it exists, melted at temperature quite similar to the bulk and could not be resolved.

The temperatures and enthalpies of the monolayer transitions are given in Table 4. The values for the adsorbed layer and bulk transition temperatures are peak maximum and on-set values, respectively. The bulk transition temperature was similar to those obtained in the literature for the pure liquid acids, similarly, as observed for alkanes and alcohols adsorbed onto graphite [6,32,33, 34]. The monolayer transition temperature increases as the number of hydroxyl groups increases in

the alkyl chain, however, the temperature difference between bulk and monolayer decreases. This decrease (in the temperature difference between bulk and monolayer transition temperatures with increasing numbers of hydroxyl groups) is compatible with the observation of a single, wide DSC peak for the 9,10-dihydroxystearic acid system but it does not conclusively demonstrate that the melting transition temperature is independent of the bulk. The enthalpies of the monolayer transitions at higher coverage, which decrease with the number of hydroxyl groups, are much smaller than the bulk melting enthalpies for each acid investigated here.

Figs. 4 - 6 show the evolution of the XRD patterns with temperature for the acid systems adsorbed onto graphite at a coverage level of 0.9 monolayers (left) and 3 monolayers (right). In general, 2D adsorbed material shows a "saw shaped" peak [35], while for a higher dimensionality, i.e. bulk, a symmetrical 3D structure peak is observed. Therefore, the bulk melting point occurs when the peaks change from a 3D shape to a 2D shape and the monolayer melting point takes place when the 2D shape peak disappears. The disappearance of the 2D XRD peaks, the monolayer melting, for 0.9 monolayers of stearic acid adsorbed onto graphite (Fig. 4, left) occurred at approximately 68 ºC. In the case of a 3-monolayer coverage, a change of 3D XRD peaks to a 2D XRD peaks was observed at 65 ºC as consequence of the bulk melting point. The 2D XRD peaks disappeared at ca. 95 ºC when the monolayer melts. For the 3-monolayer coverage, the value of the monolayer melting temperature was approximately 10% higher (in Kelvin) scale) than the bulk melting temperature and also higher than the monolayer melting for submonolayer coverage, as predicted by the literature [36].

A similar evolution of the XRD patterns was observed for the 12-hydroxystearic acid systems adsorbed onto graphite (Fig. 5), the only difference being the temperature transition as was observed with DSC. Following the explanations in the previous paragraph, from Fig. 5 we concluded that the melting point for 0.9 monolayers was approximately 58 ºC. In the case of 3 monolayers, the bulk melting point was ca. 65 ºC and the monolayer melting point was ca. 94 ºC. Similar to stearic acid, in the sample with 3 monolayers, the value of the monolayer melting temperature is approximately

10% higher (in Kelvin) than the bulk melting temperature and higher that the monolayer melting for submonolayer coverage.

A different evolution for the XRD patterns of the 9,10-dihydroxystearic acid system was observed. In the case of 0.9 monolayers adsorbed onto graphite, Fig. 6 left, the 2D XRD peaks disappeared at approximately 68 ºC and the monolayer melts. In the case of a 3 monolayer coverage (Fig. 6, right), the 3D XRD peaks disappeared at ca. 120 ºC without observation of 2D XRD peaks, as previously observed by DSC, probably due to the complete melting of the system. However, before the melting point, at ca. 78º C, the whole set of 3D XRD peaks changed their 2θ position because of a change in the structure of the acid.

3.3 Structures of acid monolayers on graphite surfaces

The STM images (Fig. 7) allowed a detailed description of the monolayer structures and the structural parameters to be calculated (Table 5). The structural parameters showed that the monolayer structures are uniaxial commensurate on the graphite surface along the *a*-axis, $6\sqrt{3}$ for stearic acid and 9,10-dihydroxystearic acid and $12\sqrt{3}$ for 12-hydroxystearic acid. Referring to the XRD peaks found in the literature [4] and the structural parameters calculated by STM, the 2θ position of the diffraction peaks of the planes (0,2) and (-1,2) for stearic acid have been calculated and the values obtained, 18.825º and 19.029º, agreed with the values obtained from the deconvolution of the raw XRD pattern, 18.791º and 19.514º, recorded at 25 ºC (see Fig. 4, left).

The schematic representations of the *p2* structure of stearic acid, 12-dihydroxystearic acid and 9,10-dihydroxystearic acid were drawn using starting data taken from the structural parameters of shorter chain carboxylic acids adsorbed onto graphite reported in the literature [4]. For this calculation, the atom positions for stearic acid were deduced from the fractional coordinates for a single repeating motif published for undecanoic acid [4] with a *pgg* structure. The molecular structure was stretched and filled-out up to an eighteen-carbon chain with the corresponding hydrogen and oxygen atom positions for stearic acid 12-hydroxystearic acid and 9,10-

dihydroxystearic acid. As was reported in the literature [23], 12-hydroxystearic acid presented a non-interdigitised dimer structure, however, stearic acid and 9,10-dihydroxystearic acid formed interdigitised dimer structures.

Finally, the superimposition of the schematic illustration of the *p2* structure for stearic acid (Fig. 7a), 12-hydroxystearic acid (Fig. 7b) and 9,10-dihydroxystearic acid (Fig. 7c) have confirmed that the calculated structures were correct. The self-assembly of the acids on the graphite surface implied that the monolayer structures did not maintain their correlation with the view of the structure from *a*-xis or *b*-axis of the carboxylic acids used for the preparation. The more related 3D structures with different monolayers were the polymorph A for the stearic acid and 9,10-dihydroxystearic acid and polymorph E_m for 12-hydroxystearic acid [37]. Analysis of the degree of molecular packing in the *ac* or *bc* plane of the 3D polymorph was performed, choosing the plane that exhibited a packing degree closest to the 2D structure and provided a rectangular cell (Table 6). The results highlighted that stearic acid and 9,10-dihydroxystearic acid exhibit the most compact structure; possibly due to the absence of -OH groups or, for the latter, due to geometrical factors caused by the proximity of both -OH groups complicating hydrogen bonding between neighboring molecules. Rabe and Buchholz [10] have already observed that carboxylic acids adsorbed in parallel monolayers onto the graphite surface provoke at least a 10% contraction of the monolayer unit cell in comparison with that of a bulk level.

4. Conclusions

The influence of hydroxyl groups on the formation and structure of carboxylic acid monolayers on graphite surfaces has been demonstrated. This influence has been explained as a consequence of the combination of the geometrical factors and hydrogen bonding between the -OH groups of neighboring molecules. Moreover, the combination of VTXRD and STM has allowed a comparison of the monolayer structure of hydroxystearic acids on recompressed and monocrystalline graphite.

The DSC and VTXRD results demonstrated the presence, in the case of stearic acid and 12-hydroxystearic acid, of a monolayer with a melting temperature 10% higher than the melting temperature of the bulk. The independent melting of a monolayer has not been demonstrated in the case of 9,10-dihydroxystearic acid, where the entire system melted at the same temperature, with a 3D structure change before the melting point.

Independent of the presence of the hydroxyl groups, the monolayer structure of the acids showed rectangular *p2* unit cells that were uniaxially commensurate in the *a*-axis. However, the 2D structures were not structurally correlated to the polymorphs described in the starting materials.

Acknowledgments

We would like to thank the DGICYT and FEDER funds (project no. CTQ 2010-14874 and CTQ 2011-24299) for their financial support.

References

[1] D.C. Duffy, A. Friedmann, S.A. Boggis and D. Klenerman, Langmuir 14 (1998) 6518.

[2] G.I. Andrews, N. Hairs, A.J. Groszek, Am. Soc. Lubric. Trans. 15 (1972) 184.

[3] A.J. Groszek, Proc. R. Soc. Lond. Ser. A 314 (1970) 473.

[4] A.K Bickerstaffe, N.P Cheah, S.M Clarke, J.E Parker, A. Perdigon, L Messe and A. Inaba, J. Phys. Chem. B 110 (2006) 5570.

[5] G.H. Findenegg, J. Chem. Soc., Faraday Trans. I 68 (1972) 1799.

[6] G.H. Findenegg, J. Chem. Soc., Faraday Trans.1 169 (1973) 1069.

[7] M. Hibino, A. Sumi, H. Tsuchiya and I. Hatta, J. Phys. Chem. B 102 (1998) 4544.

[8] M. Hibino, A. Sumi and I. Hatta, Jpn. J. Appl. Phys. 34 (1995) 3354.

[9] I. Hatta, J. Nishino, A. Sumi, A. and M. Hibino, Jpn. J. Appl. Phys. 34 (1995) 3930.

[10] J.P Rabe and S. Buchholz, Science 253 (1991) 424.

[11] M.D. Alba, A.K.Bickerstaffe, M.A.Castro, S.M Clarke, S. Medina, C. Millán, M.M Orta, E. Pavón and A.C. Perdigón, Eur. Phys. J. 167 (2009) 151.

[12] (a) D.M. Cyr, B. Venkataraman, G.M. Flynn, Chem. Mater. 8 (1996) 1600. (b) F. Tao, J. Goswami, S.L. Bernasek, J. Phys. Chem. B 110 (2006) 4199.

[13] S. De Feyter, A. Gesquiere, M.M. Abdel-Mottaleb, P.C.M. Grim, F.C. De Schryver, C. Meiners, M. Sieffert, S. Valiyaveettil, K. Mullen, Acc. Chem. Res. 33 (2000) 520.

[14] F. Tao, J. Goswami, S.L. Bernasek, J. Phys. Chem. B 110 (2006) 4199.

[15] S. De Feyter, F.C. De Schryver, Chem. Soc. Rev. 32 (2003) 139.

[16] S. De Feyter, F.C. De Schryver, J. Phys. Chem. B 109 (2005) 4290.

[17] D.B. Amabilino, S. De Feyter, R. Lazzaroni, E. Gomar-Nadal, J. Veciana, C. Rovira, M.M. Abdel-Mottaleb, W. Mamdouh, P. Iavicoli, K. Psychogyiopoulou, M. Linares, A. Minoia, H. Xu, J. Puigmarti-Luis, J. Phys.: Condens. Matter 20 (2008) 184003.

[18] E.P. Gilbert, P.A. Reynolds, J.A. White, J. Chem. Soc., Faraday Trans. 94 **(**1998) 1861.

[19] A.J. Groszek, Proc. R. Soc. London A 413 (1970) 473.

[20] K. Morishige, T.J. Kato, Chem. Phys. 111 (1999) 7095.

[21] M.D. Alba, A.K. Bickerstaffe, M.A. Castro, S.M. Clarke, S. Medina, C. Millán, M.M. Orta, E. Pavón, A. Perdigón, Eur. Phys. J. Special Topics 167 (2009) 151.

[22] D. Joseph, R. Menczel, B. Prime, Thermal analysis of polymers: fundamentals and applications, John Wiley & Sons: New Jersey, (2009).

[23] P. Qian, H. Nanjo, T. Yokoyama, T.M. Suzuki, Chem. Commun. (1999) 1197.

[24] A. Le Bail, A. Powder Diffraction. 20 (2005) 316.

[25] TOPAS 4.2 User Manual. Bruker. (2009).

[26] F. Kaneko, H. Sakashita, M. Kobayshi, Acta Crystallogr., Sect. C: Cryst. Struct. Commun. C 50 (1994) 245.

[27] T. Kamijo, H. Nagase, T. Endo, H. Ueda M. Nakagaki, Analytical Sciences. 15 (1999) 1291.

[28] F. Kaneko, H. Sakashita, M. Kobayshi, Acta Crystallogr., Sect. C: Cryst. Struct. Commun. C 50 (1994) 247.

[29] R.A. Young (Ed.): The Rietveld method; IUCr Monographs on Crystallography no 5; Oxford University Press; New York. (1993).

[30] V. Malta, G. Celotti, R. Zannetti, A.F. Martelli, J. Chem. Soc. B (1971) 548.

[31] F. Kaneko, M. Kobayashi, Y. Kitagawae , Y. Matsuura, Acta Crystallogr., Sect. C: Cryst. Struct. Commun. 46 (1990) 1490.

[32] K.W. Herwig, B. Matthies, H. Taub, Phys. Rev. Letters. 75 (1995) 3154.

[33] P. Espeau, P.A. Reynolds, T. Dowling, D. Cookson, J.W. White, J. Chem. Soc., Faraday Trans. 93 (1997) 3201.

[34] G.S. Wang, S. Lei, S. De Feyter, R. Feldman, J.E. Parker, S.M. Clarke, Langmuir 24 (2008) 2501.

[35] B.E. Warrem, Phys. Rev. 59 (1941) 693.

[36] M.A. Castro, S.M. Clarke and A. Inaba, *J. Phys. Chem. B* 1997, **101**, 8878-8882

[37] S. Medina, PhD Thesis, University of Sevilla, (2012).

Table. 1. Unit cell parameters of stearic acid after different treatments.

Sample	Polym.	Spatial group	a (Å)	b (Å)	c (Å)	β (º)	Cell unit Volume ($Å^3$)
raw	B_o	*Pbca*	7.36339(60)	5.52351(56)	87.7820(39)	--	3570.25(49)
heated	C	$P2_1/a$	9.32000(73)	4.97311(24)	50.3169(42)	127.5713(52)	1848.46(26)
solved	C	$P2_1/a$	9.3805(22)	4.9873(10)	50.858(12)	128.1989(56)	1869.80(73)
heated / solved	B_o	*Pbca*	7.43609(23)	5.58196(19)	88.6659(29)	--	3680.34(21)
	C	$P2_1/a$	9.37962(90)	4.97941(52)	50.9474(48)	128.2427(65)	1868.85(36)

Table 2. Unit cell parameters of 12-hydroxystearic acid after different treatments.

Sample	Polym.	Spatial group	a (Å)	b (Å)	c (Å)
raw	A	*P1*	8.03054(65)	48.3912(44)	4.85065(36)
heated	A	*P1*	8.1768(35)	48.784(22)	4.9119(22)
solved	A	*P1*	8.1459(20)	49.540(12)	4.9601(11)
heated / solved	A	*P1*	8.0657(10)	48.4096(60)	4.89313(62)

Sample	α (º)	β (º)	γ (º)	Cell unit Volume ($Å^3$)
raw	91.0581(70)	90.052(10)	104.9511(73)	1820.84(27)
heated	91.229(15)	90.616(24)	105.692(12)	1885.6(14)
solved	90.5349(84)	91.4609(90)	105.1133(89)	1931.50(81)
heated / solved	90.6138(38)	90.5938(47)	105.1308(41)	1844.04(40)

Table 3. Unit cell parameters of 9,10 dihydroxystearic acid after different treatments.

Sample	Polym.	Spatial group	a (Å)	b (Å)	c (Å)	β (º)	Cell unit Volume ($Å^3$)
raw	E_o	*Pbca*	7.26799(53)	5.64513(38)	83.7057(34)	--	3434.34(37)
heated	C	$P2_1/a$	9.36114(65)	4.96706(22)	50.6083(38)	127.8708(50)	1857.57(24)
solved	E_o	*Pbca*	7.38007(71)	5.73232(56)	83.5647(63)	--	3535.20(55)
heated / solved	E_m	$P2_1/a$	5.60451(12)	7.40538(15)	49.8449(10)	117.2708(13)	1843.952(77)
	C	$P2_1/a$	9.35621(22	4.97341(12)	50.8273(12)	128.2263(13)	1857.963(83)

Table 4. Temperatures and enthalpies of transitions of the bulk and monolayer of pure acids at coverage of approximately 60 monolayers.[a]

Samples	T_{3D}^{lit} (ºC)	T_{3D}^{DSC} (ºC)	T_{2D}^{DSC} (ºC)	ΔH_{2D} (J/g)
Stearic acid	67-72	67.0 69.4	95.8	0.682
12-hydroxystearic acid	74-76	79.6	100.8	0.598
9,10-dihydroxystearic acid	--	127.2 129.5	--	--

[a] T_{2D}^{DSC} monolayer transition temperature, T_{3D}^{DSC} "bulk" transition temperature from DSC, T_{3D}^{lit}, literature value of bulk melting point, and ΔH_{2D} monolayer transition enthalpy

Table 5. Structural parameters for the adsorbed monolayers of the stearic acid, the 12-hydroxystearic acid and the 9,10-dihydroxystearic acid.

Samples	a (nm)	b (nm)	ν (º)	tilt (º)	2D structure
Stearic acid	2.50	0.94	94	-6	p2
12-hydroxystearic acid	5.10	0.50	97	0	p2
9,10-dihydroxystearic acid	2.60	1.06	94	-6	p2

Table 6. Total area, molecule amount for unit cell and packing degree.

Sample	structure	Plane angle	Area ($Å^2$)	Z	Molec. per area unit (molec/$Å^2$)x10^2
Stearic acid	Polymorph C	β	374.92	4	1.07
	2D p2	ν	234.43	2	0.85
	Polymorph A	α	245.71	2	0.81
12-hydroxystearic acid	Polymorph A	α	245.71	2	0.81
	2D p2	ν	278.41	4	1.44
	Polymorph E_m	β	248.31	4	1.61
9,10-dihydroxystearic acid	Polymorph E_o	β	616.71	8	1.30
	2D p2	ν	311.24	2	0.64
	Polymorph A	α	245.71	2	0.81

FIGURE CAPTIONS

Fig. 1. XRD diffraction of pure stearic acid (a, upper), 12-hydroxystearic acid (b, middle) and 9,10-dihydroxystearic acid (c, bottom): 1) as provided, 2) after heating at 150 ºC, 3) after drying at 25 ºC a 5-10 $mg \cdot cm^{-3}$ solution of the *1* component in octanol or phenyloctane, and, 4) after drying at 25 ºC a 5-10 $mg \cdot cm^{-3}$ solution of the *2* component in octanol or phenyloctane.

Fig. 2. XRD patterns of stearic acid solved in phenyloctane and heated at 150 ºC (upper) and 9,10-dihydroxystearic acid solved in octanol and heated at 150 ºC (bottom) as dried (a) and after 30 days at 25 ºC (b).

Fig. 3. DSC thermograms for approximately 60 monolayers of stearic acid (a), 12-hydroxystearic acid (b) and 9,10-dihydroxystearic acid adsorbed on graphite.

Fig. 4. Experimental VT XRD patterns (points) and best fitting functions (lines) for 0.9 monolayers (left) and 3 monolayers (right) of stearic acid adsorbed on graphite. For 3 monolayers, bulk melting point is observed at *b*, and in both cases the melting point of the monolayer is observed at *a* and *c* respectively.

Fig. 5. Experimental VT XRD patterns (points) and best fitting functions (lines) for 0.9 monolayers (left) and 3 monolayers (right) of 12-hydroxystearic acid adsorbed on graphite. For 3 monolayers, bulk melting point is observed at *b*, and in both cases the melting point of the monolayer is observed at *a* and *c* respectively.

Fig. 6. Experimental VT XRD patterns (points) and best fitting functions (lines) for 0.9 monolayers (left) and 3 monolayers (right) of 9,10-dihydroxystearic acid adsorbed on graphite. For 3 monolayers, phase change is observed at *b* and bulk melting point at *c*. For 0.9 monolayers, melting point of the monolayer is observed at *a*.

Fig. 7. Obtained STM images and the superimposition of the schematic illustration of the *p2* structure for stearic acid (a), 12-hydroxystearic acid (b) and 9,10-dihydroxystearic acid (c).

Figure 1

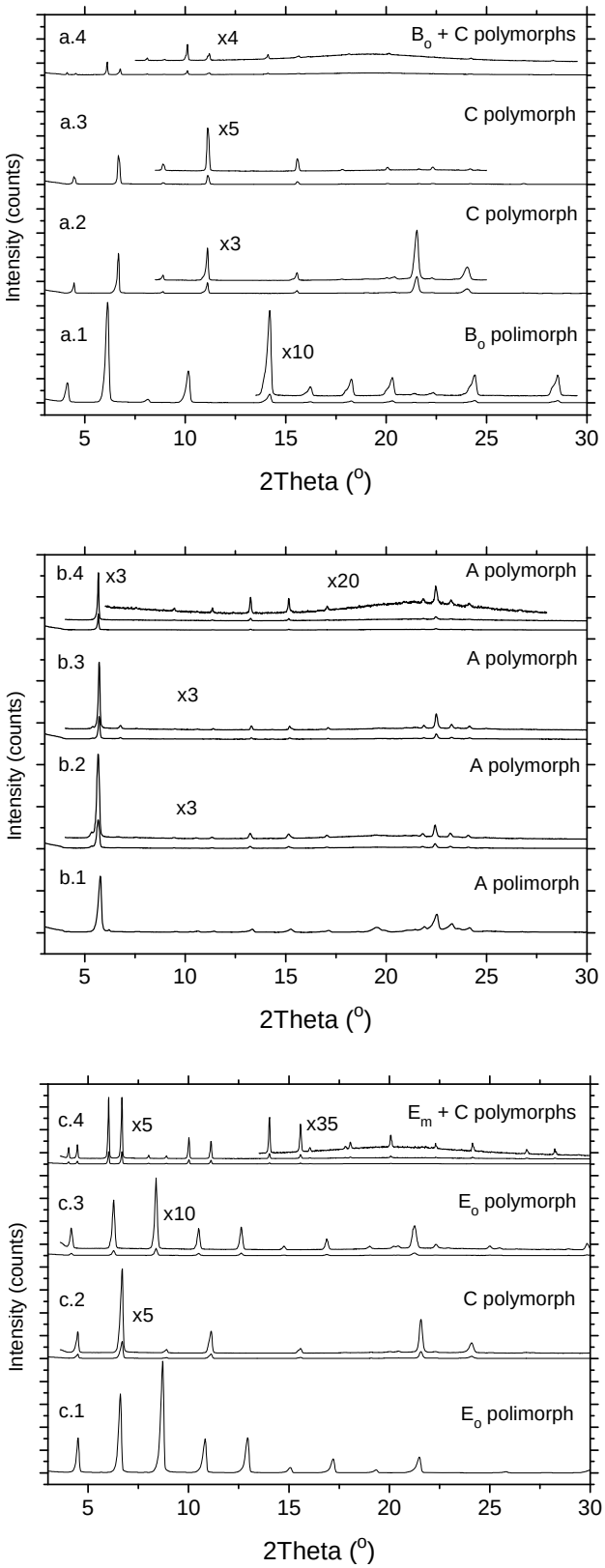
a.4
x4
B_o + C polymorphs
a.3
x5
C polymorph
a.2
x3
C polymorph
a.1
x10
B_o polimorph
Intensity (counts)
5
10
15
20
25
30
2Theta (^{o})
b.4
x3
x20
A polymorph
b.3
x3
A polymorph
b.2
x3
A polymorph
b.1
A polimorph
Intensity (counts)
5
10
15
20
25
30
2Theta (^{o})
c.4
x5
x35
E_m + C polymorphs
c.3
x10
E_o polymorph
c.2
x5
C polymorph
c.1
E_o polimorph
Intensity (counts)
5
10
15
20
25
30
2Theta (^{o})

Figure 2

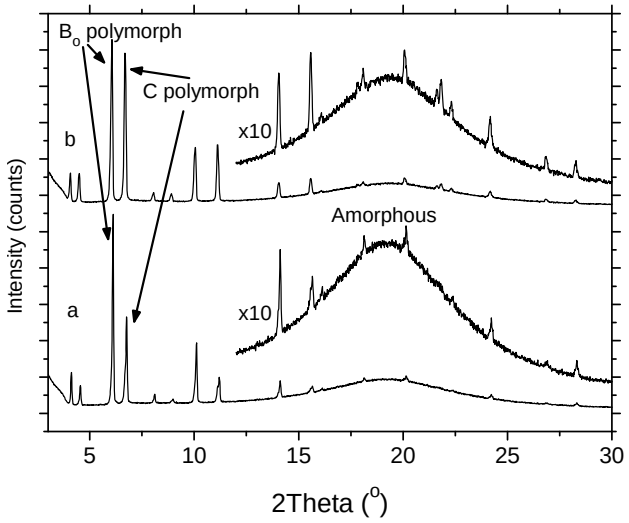
B$_o$ polymorph
C polymorph
b
x10
Amorphous
a
x10
Intensity (counts)
5
10
15
20
25
30
2Theta (^{o})

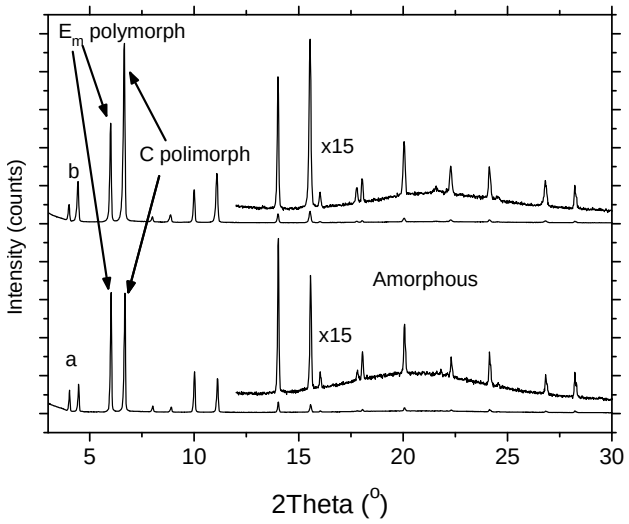
E$_m$ polymorph
C polimorph
b
x15
Amorphous
x15
a
Intensity (counts)
5
10
15
20
25
30
2Theta (^{o})

Figure 3

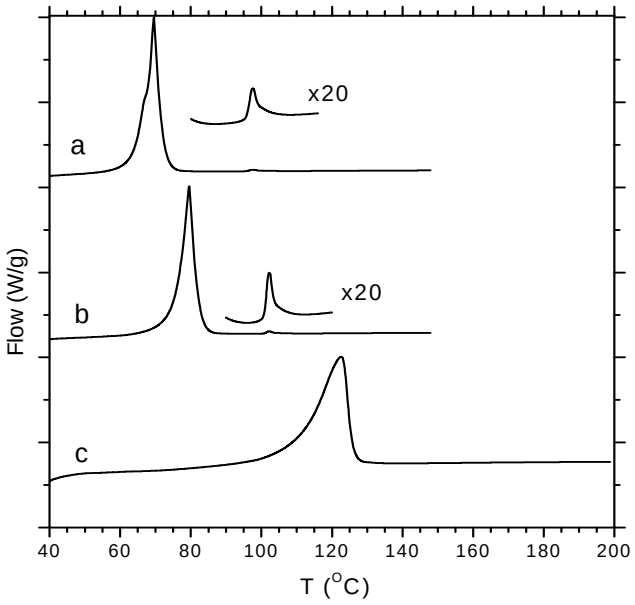

Figure 4

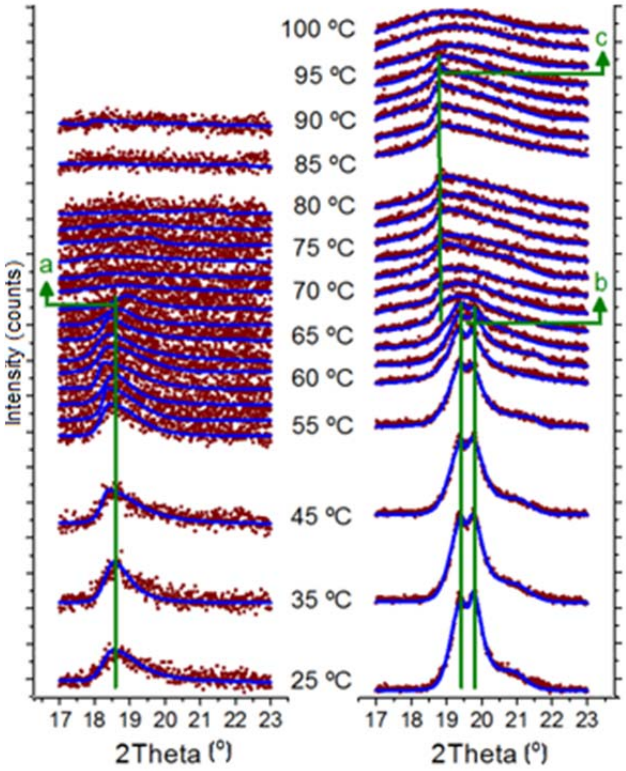
100 °C
95 °C
90 °C
85 °C
80 °C
75 °C
70 °C
65 °C
60 °C
55 °C
45 °C
35 °C
25 °C
a
b
c
Intensity (counts)
17 18 19 20 21 22 23
2Theta (°)
17 18 19 20 21 22 23
2Theta (°)

Figure 5

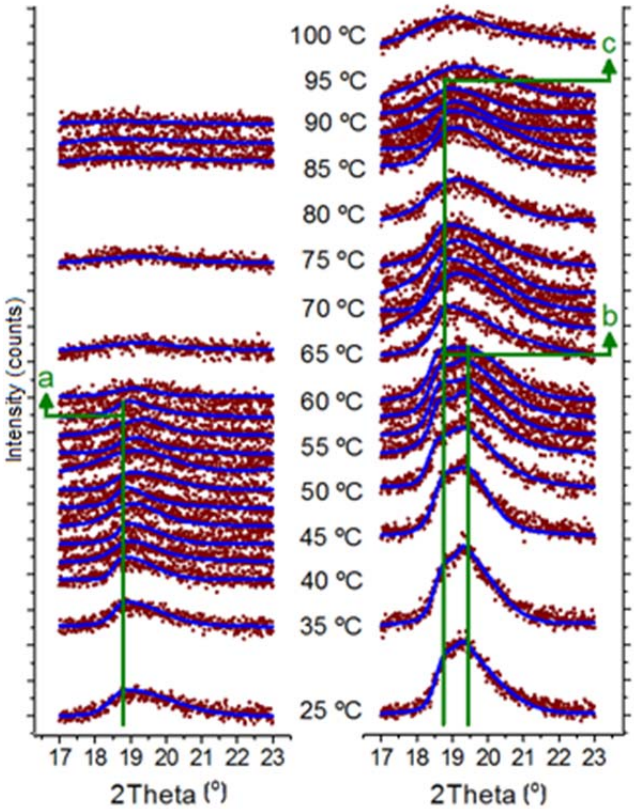
Intensity (counts)
100 °C
95 °C
90 °C
85 °C
80 °C
75 °C
70 °C
65 °C
60 °C
55 °C
50 °C
45 °C
40 °C
35 °C
25 °C
a
b
c
17 18 19 20 21 22 23
2Theta (°)
17 18 19 20 21 22 23
2Theta (°)

Figure 6

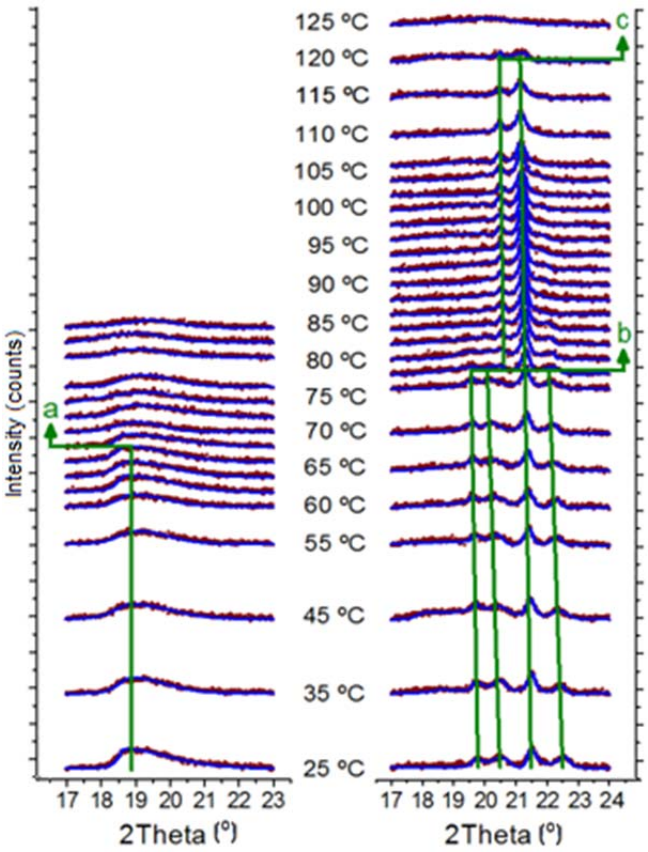
Intensity (counts)
125 °C
120 °C
115 °C
110 °C
105 °C
100 °C
95 °C
90 °C
85 °C
80 °C
75 °C
70 °C
65 °C
60 °C
55 °C
45 °C
35 °C
25 °C
a
b
c
17 18 19 20 21 22 23
2Theta (°)
17 18 19 20 21 22 23 24
2Theta (°)

Figure 7